arXiv:hep-ex/0307084v2 27 Nov 2003

Measurement of the $e^+e^- \to D^{(*)+}D^{(*)-}$ cross-sections

K. Abe,[9] K. Abe,[44] N. Abe,[47] R. Abe,[30] T. Abe,[9] I. Adachi,[9] Byoung Sup Ahn,[16]
H. Aihara,[46] M. Akatsu,[23] M. Asai,[10] Y. Asano,[51] T. Aso,[50] V. Aulchenko,[2] T. Aushev,[13]
S. Bahinipati,[5] A. M. Bakich,[41] Y. Ban,[34] E. Banas,[28] S. Banerjee,[42] A. Bay,[19]
I. Bedny,[2] P. K. Behera,[52] I. Bizjak,[14] A. Bondar,[2] A. Bozek,[28] M. Bračko,[21, 14]
J. Brodzicka,[28] T. E. Browder,[8] M.-C. Chang,[27] P. Chang,[27] Y. Chao,[27] K.-F. Chen,[27]
B. G. Cheon,[40] R. Chistov,[13] S.-K. Choi,[7] Y. Choi,[40] Y. K. Choi,[40] M. Danilov,[13]
M. Dash,[53] E. A. Dodson,[8] L. Y. Dong,[11] R. Dowd,[22] J. Dragic,[22] A. Drutskoy,[13]
S. Eidelman,[2] V. Eiges,[13] Y. Enari,[23] D. Epifanov,[2] C. W. Everton,[22] F. Fang,[8] H. Fujii,[9]
C. Fukunaga,[48] N. Gabyshev,[9] A. Garmash,[2, 9] T. Gershon,[9] G. Gokhroo,[42] B. Golob,[20, 14]
A. Gordon,[22] M. Grosse Perdekamp,[36] H. Guler,[8] R. Guo,[25] J. Haba,[9] C. Hagner,[53]
F. Handa,[45] K. Hara,[32] T. Hara,[32] Y. Harada,[30] N. C. Hastings,[9] K. Hasuko,[36]
H. Hayashii,[24] M. Hazumi,[9] E. M. Heenan,[22] I. Higuchi,[45] T. Higuchi,[9] L. Hinz,[19]
T. Hojo,[32] T. Hokuue,[23] Y. Hoshi,[44] K. Hoshina,[49] W.-S. Hou,[27] Y. B. Hsiung,[27, *]
H.-C. Huang,[27] T. Igaki,[23] Y. Igarashi,[9] T. Iijima,[23] K. Inami,[23] A. Ishikawa,[23] H. Ishino,[47]
R. Itoh,[9] M. Iwamoto,[3] H. Iwasaki,[9] M. Iwasaki,[46] Y. Iwasaki,[9] H. K. Jang,[39] R. Kagan,[13]
H. Kakuno,[47] J. Kaneko,[47] J. H. Kang,[55] J. S. Kang,[16] P. Kapusta,[28] M. Kataoka,[24]
S. U. Kataoka,[24] N. Katayama,[9] H. Kawai,[3] H. Kawai,[46] Y. Kawakami,[23] N. Kawamura,[1]
T. Kawasaki,[30] N. Kent,[8] A. Kibayashi,[47] H. Kichimi,[9] D. W. Kim,[40] Heejong Kim,[55]
H. J. Kim,[55] H. O. Kim,[40] Hyunwoo Kim,[16] J. H. Kim,[40] S. K. Kim,[39] T. H. Kim,[55]
K. Kinoshita,[5] S. Kobayashi,[37] P. Koppenburg,[9] K. Korotushenko,[35] S. Korpar,[21, 14]
P. Križan,[20, 14] P. Krokovny,[2] R. Kulasiri,[5] S. Kumar,[33] E. Kurihara,[3] A. Kusaka,[46]
A. Kuzmin,[2] Y.-J. Kwon,[55] J. S. Lange,[6, 36] G. Leder,[12] S. H. Lee,[39] T. Lesiak,[28]
J. Li,[38] A. Limosani,[22] S.-W. Lin,[27] D. Liventsev,[13] R.-S. Lu,[27] J. MacNaughton,[12]
G. Majumder,[42] F. Mandl,[12] D. Marlow,[35] T. Matsubara,[46] T. Matsuishi,[23]
H. Matsumoto,[30] S. Matsumoto,[4] T. Matsumoto,[48] A. Matyja,[28] Y. Mikami,[45]
W. Mitaroff,[12] K. Miyabayashi,[24] Y. Miyabayashi,[23] H. Miyake,[32] H. Miyata,[30]
L. C. Moffitt,[22] D. Mohapatra,[53] G. R. Moloney,[22] G. F. Moorhead,[22] S. Mori,[51] T. Mori,[47]
J. Mueller,[9, †] A. Murakami,[37] T. Nagamine,[45] Y. Nagasaka,[10] T. Nakadaira,[46] E. Nakano,[31]
M. Nakao,[9] H. Nakazawa,[9] J. W. Nam,[40] S. Narita,[45] Z. Natkaniec,[28] K. Neichi,[44]
S. Nishida,[9] O. Nitoh,[49] S. Noguchi,[24] T. Nozaki,[9] A. Ogawa,[36] S. Ogawa,[43] F. Ohno,[47]
T. Ohshima,[23] T. Okabe,[23] S. Okuno,[15] S. L. Olsen,[8] Y. Onuki,[30] W. Ostrowicz,[28]
H. Ozaki,[9] P. Pakhlov,[13] H. Palka,[28] C. W. Park,[16] H. Park,[18] K. S. Park,[40] N. Parslow,[41]
L. S. Peak,[41] M. Pernicka,[12] J.-P. Perroud,[19] M. Peters,[8] L. E. Piilonen,[53] F. J. Ronga,[19]
N. Root,[2] M. Rozanska,[28] H. Sagawa,[9] S. Saitoh,[9] Y. Sakai,[9] H. Sakamoto,[17] H. Sakaue,[31]
T. R. Sarangi,[52] M. Satapathy,[52] A. Satpathy,[9, 5] O. Schneider,[19] S. Schrenk,[5]
J. Schümann,[27] C. Schwanda,[9, 12] A. J. Schwartz,[5] T. Seki,[48] S. Semenov,[13] K. Senyo,[23]
Y. Settai,[4] R. Seuster,[8] M. E. Sevior,[22] T. Shibata,[30] H. Shibuya,[43] M. Shimoyama,[24]
B. Shwartz,[2] V. Sidorov,[2] V. Siegle,[36] J. B. Singh,[33] N. Soni,[33] S. Stanič,[51, ‡] M. Starič,[14]
A. Sugi,[23] A. Sugiyama,[37] K. Sumisawa,[9] T. Sumiyoshi,[48] K. Suzuki,[9] S. Suzuki,[54]
S. Y. Suzuki,[9] S. K. Swain,[8] K. Takahashi,[47] F. Takasaki,[9] B. Takeshita,[32] K. Tamai,[9]

Y. Tamai,[32] N. Tamura,[30] K. Tanabe,[46] J. Tanaka,[46] M. Tanaka,[9] G. N. Taylor,[22]
A. Tchouvikov,[35] Y. Teramoto,[31] S. Tokuda,[23] M. Tomoto,[9] T. Tomura,[46] S. N. Tovey,[22]
K. Trabelsi,[8] T. Tsuboyama,[9] T. Tsukamoto,[9] K. Uchida,[8] S. Uehara,[9] K. Ueno,[27]
T. Uglov,[13] Y. Unno,[3] S. Uno,[9] N. Uozaki,[46] Y. Ushiroda,[9] S. E. Vahsen,[35] G. Varner,[8]
K. E. Varvell,[41] C. C. Wang,[27] C. H. Wang,[26] J. G. Wang,[53] M.-Z. Wang,[27]
M. Watanabe,[30] Y. Watanabe,[47] L. Widhalm,[12] E. Won,[16] B. D. Yabsley,[53] Y. Yamada,[9]
A. Yamaguchi,[45] H. Yamamoto,[45] T. Yamanaka,[32] Y. Yamashita,[29] Y. Yamashita,[46]
M. Yamauchi,[9] H. Yanai,[30] Heyoung Yang,[39] J. Yashima,[9] P. Yeh,[27] M. Yokoyama,[46]
K. Yoshida,[23] Y. Yuan,[11] Y. Yusa,[45] H. Yuta,[1] C. C. Zhang,[11] J. Zhang,[51] Z. P. Zhang,[38]
Y. Zheng,[8] V. Zhilich,[2] Z. M. Zhu,[34] T. Ziegler,[35] D. Žontar,[20, 14] and D. Zürcher[19]

(The Belle Collaboration)

[1]*Aomori University, Aomori*
[2]*Budker Institute of Nuclear Physics, Novosibirsk*
[3]*Chiba University, Chiba*
[4]*Chuo University, Tokyo*
[5]*University of Cincinnati, Cincinnati, Ohio 45221*
[6]*University of Frankfurt, Frankfurt*
[7]*Gyeongsang National University, Chinju*
[8]*University of Hawaii, Honolulu, Hawaii 96822*
[9]*High Energy Accelerator Research Organization (KEK), Tsukuba*
[10]*Hiroshima Institute of Technology, Hiroshima*
[11]*Institute of High Energy Physics,*
Chinese Academy of Sciences, Beijing
[12]*Institute of High Energy Physics, Vienna*
[13]*Institute for Theoretical and Experimental Physics, Moscow*
[14]*J. Stefan Institute, Ljubljana*
[15]*Kanagawa University, Yokohama*
[16]*Korea University, Seoul*
[17]*Kyoto University, Kyoto*
[18]*Kyungpook National University, Taegu*
[19]*Institut de Physique des Hautes Énergies, Université de Lausanne, Lausanne*
[20]*University of Ljubljana, Ljubljana*
[21]*University of Maribor, Maribor*
[22]*University of Melbourne, Victoria*
[23]*Nagoya University, Nagoya*
[24]*Nara Women's University, Nara*
[25]*National Kaohsiung Normal University, Kaohsiung*
[26]*National Lien-Ho Institute of Technology, Miao Li*
[27]*Department of Physics, National Taiwan University, Taipei*
[28]*H. Niewodniczanski Institute of Nuclear Physics, Krakow*
[29]*Nihon Dental College, Niigata*
[30]*Niigata University, Niigata*
[31]*Osaka City University, Osaka*
[32]*Osaka University, Osaka*
[33]*Panjab University, Chandigarh*
[34]*Peking University, Beijing*

^{35}Princeton University, Princeton, New Jersey 08545

^{36}RIKEN BNL Research Center, Upton, New York 11973

^{37}Saga University, Saga

^{38}University of Science and Technology of China, Hefei

^{39}Seoul National University, Seoul

^{40}Sungkyunkwan University, Suwon

^{41}University of Sydney, Sydney NSW

^{42}Tata Institute of Fundamental Research, Bombay

^{43}Toho University, Funabashi

^{44}Tohoku Gakuin University, Tagajo

^{45}Tohoku University, Sendai

^{46}Department of Physics, University of Tokyo, Tokyo

^{47}Tokyo Institute of Technology, Tokyo

^{48}Tokyo Metropolitan University, Tokyo

^{49}Tokyo University of Agriculture and Technology, Tokyo

^{50}Toyama National College of Maritime Technology, Toyama

^{51}University of Tsukuba, Tsukuba

^{52}Utkal University, Bhubaneswer

^{53}Virginia Polytechnic Institute and State University, Blacksburg, Virginia 24061

^{54}Yokkaichi University, Yokkaichi

^{55}Yonsei University, Seoul

Abstract

In this paper we report the first measurement of $e^+e^- \to D^{(*)+}D^{(*)-}$ processes. The cross-sections for $e^+e^- \to D^{*+}D^{*-}$ and $e^+e^- \to D^+D^{*-}$ at $\sqrt{s} = 10.58\,\mathrm{GeV}/c^2$ have been measured to be $0.65 \pm 0.04 \pm 0.07\,\mathrm{pb}$ and $0.71 \pm 0.05 \pm 0.09\,\mathrm{pb}$, respectively. We set an upper limit on the cross-section of $e^+e^- \to D^+D^-$ of $0.04\,\mathrm{pb}$ at the 90% confidence level. In addition we have measured the fraction of the $D_T^{*\pm}D_L^{*\mp}$ final state in the $e^+e^- \to D^{*+}D^{*-}$ reaction to be $(97 \pm 5)\%$. The analysis is performed using $88.9\,\mathrm{fb}^{-1}$ of data collected by the Belle detector at the e^+e^- asymmetric collider KEKB.

3

The processes $e^+e^- \to D^{(*)}\overline{D}^{(*)}$, with no extra fragmentation particles in the final state, have not previously been observed at energies $\sqrt{s} \gg 2M_D$. The cross-sections for these processes can be derived once the charmed meson form factors are determined for the appropriate value of momentum transfer, $q^2 \equiv s$. In the HQET approach based on the heavy-quark spin symmetry, the heavy meson form factors are represented in terms of a universal form factor, called the Isgur-Wise function. However, for asymptotically large $q^2 \gg M_c^3/\Lambda$ the leading-twist contribution, which violates the heavy-quark spin symmetry, becomes dominant [1]. For an intermediate range of momentum transfer, sub-leading twist corrections are also important. A calculation that takes these effects into account [1] predicts cross-sections of about $5\,\mathrm{pb}^{-1}$ for $e^+e^- \to D\overline{D}^*$ and $e^+e^- \to D_T^*\overline{D}_L^*$ at $\sqrt{s} \sim 10.6\,\mathrm{GeV}$ (the subscripts indicate transverse [T] and longitudinal [L] polarization of the D^*); the cross-section for $e^+e^- \to D\overline{D}$ is expected to be suppressed by a factor of $\sim 10^{-3}$.

In this paper, we present the first observation of the high energy $e^+e^- \to D^{*+}D^{*-}$ and $e^+e^- \to D^+D^{*-}$ processes, and a measurement of their cross-sections and polarizations. We also set an upper limit on the cross-section for $e^+e^- \to D^+D^-$.

The present study is limited to final states that contain charged $D^{(*)}$ mesons only: this simplifies the analysis, since it is possible to select events with no neutral particles in the final state. Since the contribution of electromagnetic current coupled to light quarks is negligible compared to that for heavy quarks, the neutral and charged charm cross-sections are expected to be the same [1].

The analysis is based on $88.9\,\mathrm{fb}^{-1}$ of data at the $\Upsilon(4S)$ resonance and nearby continuum, collected with the Belle detector [2] at the KEKB asymmetric energy storage rings [3]. We select well-reconstructed tracks consistent with originating from the interaction region as charged pion candidates. Those passing particle identification cuts based on dE/dx, aerogel Čerenkov, and time-of-flight information [2] are selected as charged kaon candidates. We then reconstruct D^0 and D^+ mesons in the decay modes $D^0 \to K^-\pi^+$, $D^0 \to K^-\pi^+\pi^+\pi^-$ and $D^+ \to K^-\pi^+\pi^+$. The selected combinations are constrained to a common vertex, and quality cuts are imposed on the vertex fit to reduce the combinatorial background. A $15\,\mathrm{MeV}/c^2$ interval around the nominal D masses is used to select $D^0 \to K^-\pi^+$ and $D^+ \to K^-\pi^+\pi^+$ candidates; for the $D^0 \to K^-\pi^+\pi^+\pi^-$ decay mode the signal window is chosen to be $10\,\mathrm{MeV}/c^2$ around the nominal D^0 mass. The selected D candidates are then subjected to a mass and vertex constrained fit to improve their momentum resolution. The D^{*+} mesons are reconstructed in the $D^0\pi^+$ decay mode. The invariant mass of the $D^0\pi^+$ combination is required to be within a $2\,\mathrm{MeV}/c^2$ ($\sim 3\,\sigma$) mass interval around the nominal D^{*+} mass.

The processes $e^+e^- \to D^{(*)+}D^{(*)-}$ can be identified by energy-momentum balance in fully reconstructed events that contain only a pair of charm mesons. However, the small charm meson reconstruction efficiency via the studied channels results in a very small total efficiency in this case. Taking into account two body kinematics, it is sufficient to reconstruct only one of the two charmed mesons in the event to identify the processes of interest. For simplicity, we refer to the fully reconstructed D meson as the $D^{(*)+}$, and the other as the D^{*-}; the charge-conjugate modes are included in the analysis. We choose the mass of the system recoiling against the reconstructed $D^{(*)+}$ ($M_{\mathrm{recoil}}(D^{(*)+})$) as a discriminating variable:

$$M_{\mathrm{recoil}}(D^{(*)+}) = \sqrt{(\sqrt{s} - E_{D^{(*)+}})^2 - \vec{p}_{D^{(*)+}}^{\,2}}, \qquad (1)$$

where $\sqrt{s}$ is the total center of mass (CMS) energy, and $E_{D^{(*)+}}$ and $\vec{p}_{D^{(*)+}}$ are the CMS energy and momentum of the reconstructed $D^{(*)+}$. For the signal a peak in the M_{recoil}

distribution around the nominal mass of the recoiling D^- or D^{*-} is expected. This method provides a significantly increased efficiency, but also a higher background, in comparison to full event reconstruction. For the $e^+e^- \to D^+D^{*-}$ and $e^+e^- \to D^{*+}D^{*-}$ processes we find a better compromise between higher statistics and smaller background: the first $D^{(*)+}$ is fully reconstructed, while the recoiling D^{*-} is required to decay into $\bar{D}^0\pi^-_{slow}$. The reconstructed π^-_{slow} provides extra information that allows us to reduce the background to a negligible level as explained below.

We calculate the difference between the masses of the systems recoiling against the $D^{(*)+}\pi^-_{slow}$ combination, and against the $D^{(*)+}$ alone,

$$\Delta M_{\mathrm{recoil}} \equiv M_{\mathrm{recoil}}(D^{(*)+}\pi^-_{slow}) - M_{\mathrm{recoil}}(D^{(*)+}).$$

The variable $\Delta M_{\mathrm{recoil}}$ peaks around the nominal $D^{*+} - D^0$ mass difference with a resolution of $\sigma_{\Delta M_{\mathrm{recoil}}} \sim 1\,\mathrm{MeV}/c^2$ as found by Monte Carlo simulation. For $e^+e^- \to D^{*+}D^{*-}$ and $e^+e^- \to D^+D^{*-}$ we combine D^{*+} and D^+ candidates together with π^-_{slow} and require $\Delta M_{\mathrm{recoil}}$ to be within a $\pm 2\,\mathrm{MeV}/c^2$ interval around the nominal $M_{D^{*+}} - M_{D^0}$ mass difference.

The $M_{\mathrm{recoil}}(D^{*+})$ and $M_{\mathrm{recoil}}(D^+)$ distributions are shown in Figs. 1a and 1b, respectively. Clear signals are seen around the nominal D^{*-} mass in both cases. The higher recoil mass tails in the signal distribution are due to initial state radiation (ISR). The hatched histograms show the M_{recoil} distributions for events in the $\Delta M_{\mathrm{recoil}}$ sidebands.

The backgrounds in the region of $M_{\mathrm{recoil}} < 2.1\,\mathrm{GeV}/c^2$, are negligible for both processes. To provide a numerical estimate, we divide the background sources into three categories:

I fake reconstructed D^{*+} or D^+;

II $e^+e^- \to D^{(*)+}D^{(*)}n\pi$, where the π^-_{slow} is not produced from D^{*-} decays, and, thus, produces no peak in the $\Delta M_{\mathrm{recoil}}$ distribution;

III $e^+e^- \to D^{(*)+}D^{*-}n\pi$, where $n \geq 1$.

First we consider the backgrounds for the process $e^+e^- \to D^{*+}D^{*-}$. To estimate background (I) we count the entries in the $M_{\mathrm{recoil}}(D^0\pi^+) < 2.1\,\mathrm{GeV}/c^2$ interval for $D^0\pi^+$ combinations taken from the D^{*+} mass sideband ($2.016 < M_{D^0\pi^+} < 2.02\,\mathrm{GeV}/c^2$). Three events are found in the data, while the Monte Carlo predicts a contribution of 2.5 events the from non-Gaussian tails in the $M_{D^{*+}}$ resolution function. The signal Monte Carlo is normalized to the number of entries in $M_{\mathrm{recoil}}(D^{*+}) < 2.1\,\mathrm{GeV}/c^2$ region in the data. Background (II) is estimated using $\Delta M_{\mathrm{recoil}}$ sidebands ($0.150 < \Delta M_{\mathrm{recoil}} < 0.154\,\mathrm{MeV}/c^2$). In the region $M_{\mathrm{recoil}}(D^{*+}) < 2.1\,\mathrm{GeV}/c^2$ 8 events are found in the data; according to Monte Carlo, 4 events are expected from initial state radiation. Thus, backgrounds (I) and (II) are estimated to be smaller than 3 and 9 events at 90% CL, respectively. As a cross-check we also study the wrong-sign $D^{(*)+}\pi^+_{slow}$ combinations: 2 events with wrong-sign π^+_{slow}'s are found in the data in the interval $M_{\mathrm{recoil}}(D^{*+}) < 2.1\,\mathrm{GeV}/c^2$.

The remaining background (III) can result in peaks in both the $M(D^{*+})$ and $\Delta M_{\mathrm{recoil}}$ distributions, but has a threshold in M_{recoil} distribution at $M_{D^{*+}} + M_{\pi^0} = 2.15\,\mathrm{GeV}/c^2$, which is $\sim 1\sigma$ away from the chosen $M_{\mathrm{recoil}}(D^{*+})$ interval. To estimate the residual background (III) contribution we perform a fit to the $M_{\mathrm{recoil}}(D^{*+})$ distribution. The signal function is the result of convolving the generated $M_{\mathrm{recoil}}(D^{*+})$ distribution with the detector resolution: the signal function is the sum of a core Gaussian and an asymmetric function representing the $M_{\mathrm{recoil}}(D^{*+})$ shape when the studied process is accompanied by radiative photon(s)
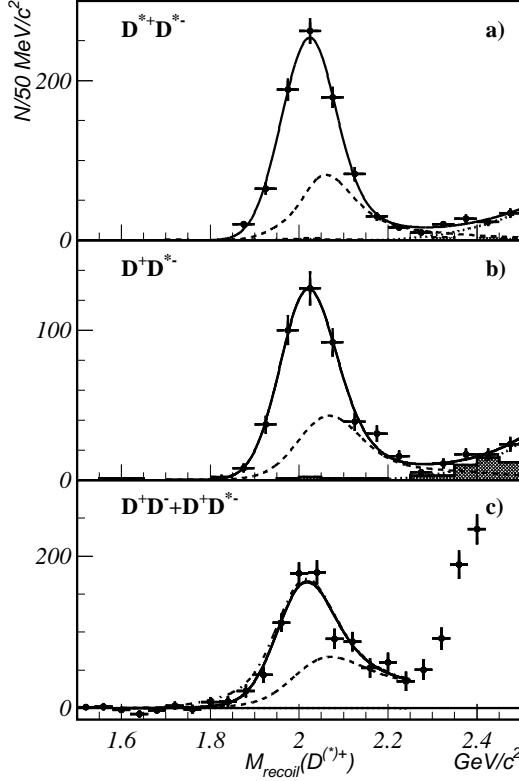
FIG. 1: a-b) The distributions of the mass of the system recoiling against a) D^{*+}, and b) D^{+}. Points with error bars show the signal $\Delta M_{\rm recoil}$ region; hatched histograms correspond to $\Delta M_{\rm recoil}$ sidebands. The solid lines represent the fits described in the text; the dashed lines show the contribution due to events with ISR photons of significant energy. The dotted lines show the expected background contribution. c) The distributions of $M_{\rm recoil}(D^{+})$ without any requirement on $\Delta M_{\rm recoil}$.

with significant energy. The $M_{\rm recoil}(D^{*+})$ resolution due to detector smearing and the signal function offset are left as free parameters in the fit, to test the agreement with the Monte Carlo predictions. The background (III) distribution is parameterized by a threshold function, $\alpha \cdot (M_{\rm recoil}(D^{*+}) - M(D^{*-})_{PDG} - M(\pi^{0})_{PDG})^{\beta}$, convolved with the detector resolution, where α and β are free parameters. The fit results are shown in Fig. 1a as the solid line. The dotted line represents the expected background (III) distribution. The signal yield is found to be 815 ± 28 events. The $M_{\rm recoil}$ resolution $\sigma = 56.1 \pm 2.2\,{\rm MeV}/c^{2}$ is found to be in excellent agreement with the Monte Carlo expectation ($56.4\,{\rm MeV}/c^{2}$), and the shift of the signal peak position in the data with respect to the Monte Carlo position is found to be consistent with zero ($0.6 \pm 2.5\,{\rm MeV}/c^{2}$). The contribution from background (III) in the $M_{\rm recoil} < 2.1\,{\rm GeV}/c^{2}$ interval is estimated from this fit to be less than 2 events.

The backgrounds for the $e^{+}e^{-} \rightarrow D^{+}D^{*-}$ process are studied in a similar way. Five events are found in the data in the D^{+} mass sideband region ($20 < |M_{K^{-}\pi^{+}\pi^{+}} - M_{D+}| < 35\,{\rm MeV}/c^{2}$), whereas 1.5 events are expected from the signal Monte Carlo. There are 6 data events in the $\Delta M_{\rm recoil}$ sidebands with $M_{\rm recoil}(D^{+}) < 2.1\,{\rm GeV}/c^{2}$, while 6 signal events are expected from the Monte Carlo simulation. Thus backgrounds (I) and (II) for the $e^{+}e^{-} \rightarrow D^{+}D^{*-}$ process are estimated to be smaller than 7 and 4 events at 90% CL,

respectively. Three wrong sign $D^+\pi^+_{slow}$ combinations are found in the data in the interval $M_{\mathrm{recoil}}(D^+) < 2.1\,\mathrm{GeV}/c^2$. A similar fit is then performed to the $M_{\mathrm{recoil}}(D^+)$ distribution. The signal yield is found to be 423 ± 20 events. Again, excellent agreement between the Monte Carlo and signal shape parameters is found: $\sigma = 58.1 \pm 3.6\,\mathrm{MeV}/c^2$ ($60\,\mathrm{MeV}/c^2$ is expected from the Monte Carlo); $M(D^{*-})_{data} - M(D^{*-})_{MC} = -2.1 \pm 3.6\,\mathrm{MeV}/c^2$. We conclude that background (III) is smaller than 2 events.

From the above study we estimate the total background in the $M_{\mathrm{recoil}} < 2.1\,\mathrm{GeV}/c^2$ interval to be smaller than 14 and 16 events for the $e^+e^- \to D^{*+}D^{*-}$ and $e^+e^- \to D^+D^{*-}$ processes, respectively, which is of order of 1% of the signal. We assume all events in the interval $M_{\mathrm{recoil}} < 2.1\,\mathrm{GeV}/c^2$ are signal and include the possible background contribution in the systematic error.

Since the reconstruction efficiency depends on the production and $D^{*\pm}$ helicity angles, we perform an angular analysis before computing cross-sections. The helicity angle of the non-reconstructed D^{*-} is calculated assuming two-body kinematics. A scatter plot of the helicity angles for the two D^*-mesons from $e^+e^- \to D^{*+}D^{*-}$ ($\cos\phi(D^*_{rec})$ vs $\cos\phi(D^*_{non-rec})$) for the recoil mass region $M_{\mathrm{recoil}}(D^{*+}) < 2.1\,\mathrm{GeV}/c^2$ is shown in Fig. 2a. The distribution is fitted by a sum of three functions corresponding to the $D^*_T D^*_T$, $D^*_T D^*_L$ and $D^*_L D^*_L$ final states, obtained from Monte Carlo simulation. The fit finds the fractions of $D^*_T D^*_T$, $D^*_T D^*_L$ and $D^*_L D^*_L$ final states to be $(1.5 \pm 3.6)\%$, $(97.2 \pm 4.8)\%$ and $(1.3 \pm 4.7)\%$, respectively. Figure 2b shows the D^{*-} meson helicity distribution for $e^+e^- \to D^+D^{*-}$. The fraction of the $D^+D^{*-}_T$ [6] final state is found from the fit to be equal to $(95.8 \pm 5.6)\%$.
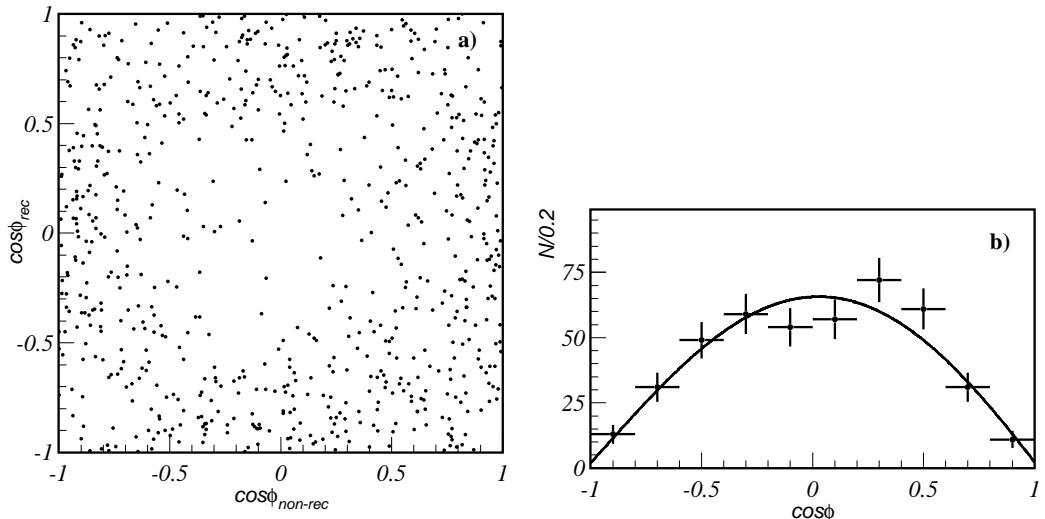

FIG. 2: a) The scatter plot $\cos(\phi_{D^*_{rec}})$ vs $\cos(\phi_{D^*_{non-rec}})$ ($e^+e^- \to D^{*+}D^{*-}$). b) D^{*+} meson helicity angle distribution for ($e^+e^- \to D^+D^{*-}$) signal candidates.

The raw production angle distributions for D^{*+} from $e^+e^- \to D^{*+}D^{*-}$ and D^+ from $e^+e^- \to D^+D^{*-}$ processes are obtained from the region of recoil masses $M_{\mathrm{recoil}} < 2.1\,\mathrm{GeV}/c^2$. In this region, the efficiency for signal events with initial state radiation photon(s) with significant energy is low. We calculate the fraction of rejected ISR events according to a Monte Carlo simulation based on Ref. [4], in bins of the production angle. The reconstruction efficiency is estimated from the Monte Carlo simulation, in the same production angle bins, taking the measured $D^{*\pm}$ polarization into account. Figures 3a and 3b show the production

angle distributions for D^{*+} from $e^+e^- \to D^{*+}D^{*-}$ and D^+ from $e^+e^- \to D^+D^{*-}$, respectively, after correcting for the reconstruction efficiencies and intermediate branching ratios. These distributions are fitted with the function $N \cdot (1 + \alpha \cos^2 \theta)$. To calculate the total cross-sections, the signal yields are corrected to take into account the fraction of events with initial state radiation that lie outside of the interval $M_{\mathrm{recoil}} < 2.1\,\mathrm{GeV}/c^2$. The efficiency corrected signal yields are found to be 58000 ± 3400 and 64000 ± 4800 for the $e^+e^- \to D^{*+}D^{*-}$ and $e^+e^- \to D^+D^{*-}$ processes respectively. The parameters α are equal to 0.8 ± 0.3 and $2.3^{+0.8}_{-0.7}$ for the two processes.
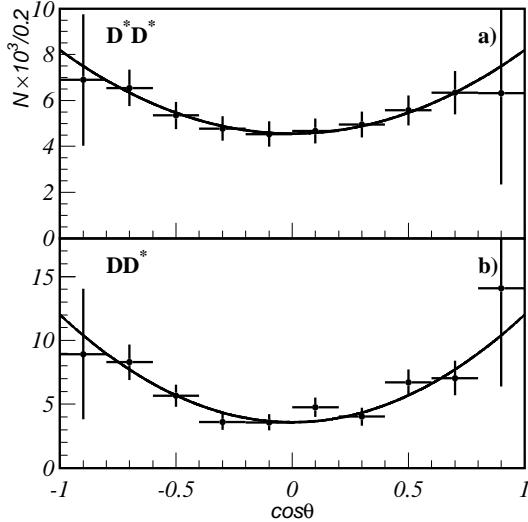
FIG. 3: The $D^{(*)+}$ production angle distribution for a) $e^+e^- \to D^{*+}D^{*-}$ and b) $e^+e^- \to D^+D^{*-}$ processes after correcting for reconstruction efficiencies and intermediate branching fractions.

We find cross-sections of $0.65 \pm 0.04 \pm 0.07\,\mathrm{pb}$ and $0.71 \pm 0.05 \pm 0.09\,\mathrm{pb}$ for $e^+e^- \to D^{*+}D^{*-}$ and $e^+e^- \to D^+D^{*-}$, respectively, where the first error is statistical and the second systematic. The sources of systematic error are summarized in Table I. The dominant contributions are from the uncertainties in tracking efficiency and corrections for the initial state radiation.

Source	$e^+e^- \to D^{*+}D^{*-}$	$e^+e^- \to D^+D^{*-}$
Tracking efficiency	9%	8%
Identification	2%	2%
Backgrounds	$^{+1}_{-0}$%	$^{+1}_{-0}$%
ISR correction	5%	5%
$\mathcal{B}(D^{(*)})$	4%	8%
Total	11%	13%

TABLE I: Contributions to the systematic error for the $e^+e^- \to D^{*+}D^{*-}$ and $e^+e^- \to D^+D^{*-}$ processes.

We search for the process $e^+e^- \to D^+D^-$ by studying the recoiling against the reconstructed D^+ (M_{recoil}). In the $e^+e^- \to D^{*+}D^{*-}$ and $e^+e^- \to D^+D^{*-}$ analyses, backgrounds

are strongly suppressed by the tight ΔM_{recoil} cut, which is not applicable dor $e^+e^- \to D^+D^-$. Without this cut the combinatorial background is significant ($\sim 20\%$). We use D^+ mass sidebands ($20 < |M_{K\pi\pi} - M_D| < 35\,\text{MeV}/c^2$) to extract the M_{recoil} distribution for the combinatorial background. Fig. 1c shows the distribution of $M_{\text{recoil}}(D^+)$ after sideband subtraction. To extract the $e^+e^- \to D^+D^-$ and $e^+e^- \to D^+D^{*-}$ yields we fit this distribution with the sum of two signal functions corresponding to D^- and D^{*-} peaks and a background function. The latter is a threshold function, $\alpha \cdot (x - M(D^-)_{PDG} - M(\pi^0)_{PDG})^\beta$, convolved with the detector resolution, where α and β are free parameters. For the fit we use only the region $M_{\text{recoil}} < 2.25\,\text{GeV}/c^2$, because of the contribution of $e^+e^- \to D^{(*)}D^{**}$ at higher M_{recoil}.

The fit finds -13 ± 24 events in the D^+ peak and 935 ± 42 in the D^{*+} peak. The fit function is shown in the Fig. 1c as the solid line; the dashed line shows the contribution of events with ISR photons of signficant energy (larger in this case due to absence of the ΔM_{recoil} cut); and the dotted line represents the case where the contribution of $e^+e^- \to D^+D^-$ is set at the value corresponding to the 90% confidence level upper limit. The reconstruction efficiencies for the $e^+e^- \to D^+D^-$ and $e^+e^- \to D^+D^{*-}$ are found from Monte Carlo to be 3.1% and 1.7%, respectively. In the $e^+e^- \to D^+D^-$ Monte Carlo the D^+ production angle is assumed to have a $\sin^2\theta$ distribution, as required by conservation of angular momentum; for $e^+e^- \to D^+D^{*-}$ the production angle distribution is fixed according to the analysis presented above. The $e^+e^- \to D^+D^{*-}$ cross-section is calculated to be $0.61 \pm 0.05\,\text{pb}$ which agrees with the result using the ΔM_{recoil} method. However, in this case the systematic uncertainty in the signal yield is large due to the non-negligible $e^+e^- \to D^+D\pi$ background under the peak, which can only be determined from the higher M_{recoil} region. For the $e^+e^- \to D^+D^-$ cross-section we set an upper limit of $0.04\,\text{pb}$ at the 90% confidence level.

In summary, we report the first measurement of the cross-sections for the $e^+e^- \to D^{*+}D^{*-}$ and $e^+e^- \to D^+D^{*-}$ processes at $\sqrt{s} = 10.6\,\text{GeV}$ to be $0.65\pm0.04\pm0.07\,\text{pb}$ and $0.71\pm0.05\pm0.09\,\text{pb}$, respectively, and set an upper limit on the $e^+e^- \to D^+D^-$ cross-section of $0.04\,\text{pb}$ at 90% confidence level. The measured cross-sections are an order of magnitude lower than those predicted in the Ref. [1], but their relative sizes are as predicted: the cross-sections for $e^+e^- \to D^{*+}D^{*-}$ and $e^+e^- \to D^+D^{*-}$ are found to be close each other, while the cross-section for $e^+e^- \to D^+D^-$ is much smaller. The helicity decomposition for $e^+e^- \to D^{*+}D^{*-}$ is found to be saturated by the $D_T^{*\pm}D_L^{*\mp}$ final state (the fraction is equal to $(97.2\pm4.8)\%$) and for $e^+e^- \to D^+D^{*-}$ – by the D_T^* final state ($95.8\pm5.6\%$), in good agreement with the predictions of Ref. [1].

* on leave from Fermi National Accelerator Laboratory, Batavia, Illinois 60510

† on leave from University of Pittsburgh, Pittsburgh PA 15260

‡ on leave from Nova Gorica Polytechnic, Nova Gorica

[1] A. G. Grozin, M. Neubert, Phys. Rev. **D55**, 272 (1997).

[2] S.Kurokawa and E.Kikutani, Nucl. Instr. and Meth. A **499**, 1 (2003).

[3] KEK accelerator group, KEKB B-Factory Design Report, KEK Report 95-7, 1995.

[4] An Introduction to Quantum Field Theory.. By Michael E. Peskin (SLAC), D.V. Schroeder (Weber State U.). 1995. Reading, USA: Addison-Wesley (1995) 842 p., Chapter 6.4 "Electron Vertex Function: Infrared Divergence"

[5] Estia Eichten, Brian Hill, Phys.Lett.B234:511,1990

[6] There was a typo in the previous draft version and in the EPS2003 presentation . "fraction of the $D^+ D_L^{*-}$" was typed. Now the text is correct.